

Enstatite-rich Warm Debris Dust around HD165014

Hideaki Fujiwara^{1*}, Takashi Onaka¹, Daisuke Ishihara², Takuya Yamashita³,
Misato Fukagawa⁴, Takao Nakagawa⁵, Hirokazu Kataza⁵, Takafumi Ootsubo⁶, and
Hiroshi Murakami⁵

ABSTRACT

We present the *Spitzer*/Infrared Spectrograph spectrum of the main-sequence star HD165014, which is a warm ($\gtrsim 200$ K) debris disk candidate discovered by the *AKARI* All-Sky Survey. The star possesses extremely large excess emission at wavelengths longer than $5\ \mu\text{m}$. The detected flux densities at 10 and $20\ \mu\text{m}$ are ~ 10 and ~ 30 times larger than the predicted photospheric emission, respectively. The excess emission is attributable to the presence of circumstellar warm dust. The dust temperature is estimated as 300–750 K, corresponding to the distance of 0.7–4.4 AU from the central star. Significant fine-structured features are seen in the spectrum and the peak positions are in good agreement with those of crystalline enstatite. Features of crystalline forsterite are not significantly seen. HD165014 is the first debris disk sample that has enstatite as a dominant form of crystalline silicate rather than forsterite. Possible formation of enstatite dust from differentiated parent bodies is suggested according to the solar system analog. The detection of an enstatite-rich debris disk in the current study suggests the presence of large bodies and a variety of silicate dust processing in warm debris disks.

Subject headings: circumstellar matter — zodiacal dust — infrared: stars — stars: individual (HD165014)

¹Department of Astronomy, School of Science, University of Tokyo, Bunkyo-ku, Tokyo 113-0033, Japan; hideaki@ir.isas.jaxa.jp

²Graduate School of Science, Nagoya University, Furo-cho, Chikusa-ku, Nagoya 464-8602, Japan

³National Astronomical Observatory of Japan, 2-21-1 Osawa, Mitaka, Tokyo 181-0015, Japan

⁴Graduate School of Science, Osaka University, 1-1 Machikaneyama, Toyonaka 560-0043, Osaka, Japan

⁵Institute of Space and Astronautical Science, Japan Aerospace Exploration Agency, 3-1-1 Yoshinodai, Chuo-ku, Sagami-hara, Kanagawa 252-5210, Japan

⁶Astronomical Institute, Graduate School of Science, Tohoku university, Aramaki, Aoba-ku, Sendai, 980-8578, Japan

1. Introduction

Debris disks were discovered in main-sequence stars by infrared excess over the photospheric emission in observations by *IRAS* in the 1980s. Since debris disks are thought to be “extra-solar zodiacal light” formed via dust production from asteroids and/or comets (e.g. Backman & Paresce 1993; Lecavelier Des Etangs et al. 1996), it is interesting to examine mineralogical characteristics of debris dust and to explore connection between the debris dust and the dust in the solar system. Debris disks are also important as a probe of planetesimals, building blocks of planets, in extra-solar systems.

Mid-infrared (MIR) spectroscopy is a strong tool to investigate the properties of debris dust. Recent MIR observations with InfraRed Spectrograph (IRS; Houck et al. 2004) on board *Spitzer* (Werner et al. 2004) have revealed the presence of abundant crystalline forsterite (Mg_2SiO_4) and silica (SiO_2) in several debris disks (e.g. Chen et al. 2006; Lisse et al. 2009).

In this Letter, we present an MIR low resolution spectrum of the main-sequence star HD165014 obtained with *Spitzer*/IRS. HD165014 is a debris disk candidate with large MIR excess selected from a search for debris disks (Fujiwara et al. 2010) in the *AKARI*/Infrared Camera (IRC) All-Sky Survey data (Ishihara et al. 2010). We report the detection of abundant crystalline enstatite (MgSiO_3) dust compared to forsterite toward the star and discuss the origin of the debris dust around HD165014.

2. Observations and Data Analysis

2.1. *AKARI*/IRC all-sky survey

The S9W (9 μm) and L18W (18 μm) images of HD165014 were taken with the IRC (Onaka et al. 2007) on board *AKARI* (Murakami et al. 2007) as part of the All-Sky Survey observations from 2006 May to 2007 August (Ishihara et al. 2010). The 5σ sensitivity for a point source per scan is estimated to be 50 mJy in the S9W band and 90 mJy in the L18W band, and the typical absolute uncertainty in flux density is $\sim 3\%$ for the S9W band and $\sim 4\%$ for the L18W band at present. HD165014 was observed twice in the survey with the interval of 6 months and the fluxes at the two periods agree with each other within the uncertainty, indicating no significant variations in the flux. The position accuracy and

*present address: Institute of Space and Astronautical Science, Japan Aerospace Exploration Agency, 3-1-1 Yoshinodai, Chuo-ku, Sagami-hara, Kanagawa 252-5210, Japan

spatial resolution is estimated to be better than $2''$ and $10''$, respectively, securely concluding that the *AKARI* source is associated with HD165014. HD165014 was selected as a candidate of warm debris disk with large $18\ \mu\text{m}$ excess by a search in the *AKARI*/IRC All-Sky Survey data (Fujiwara et al. 2010).

2.2. *Spitzer*/IRS Observations

IRS observations of HD165014 were made on 2008 November 5 (AOR ID 26122752). All the four low-resolution modules, Short-Low 2 (SL2; $5.2\text{--}7.7\ \mu\text{m}$) and Short-Low 1 (SL1; $7.4\text{--}14.5\ \mu\text{m}$), Long-Low 2 (LL2; $14.0\text{--}21.3\ \mu\text{m}$) and Long-Low 1 (LL1; $19.5\text{--}38.0\ \mu\text{m}$), were used to obtain a full $5\text{--}35\ \mu\text{m}$ low-resolution ($\lambda/\Delta\lambda \sim 100$) spectrum. We use the pipeline-processed (S18.1) Basic Calibrated Data products from the *Spitzer* Science Center and analyzed the sky-subtracted extracted one-dimensional spectral data “bksub.tbl” since the target is a point source in a relatively empty field. The wavelength calibration is as good as $0.1\ \mu\text{m}$ along the dispersal direction. For the LL1 spectra, we use the data only for $\lambda < 35\ \mu\text{m}$ because the noise becomes large at $\lambda > 35\ \mu\text{m}$, whose spectral range is not crucial for the present analysis. The absolute flux accuracy in the SL and LL spectra of the pipeline-processed products is better than 10%.

2.3. Subaru/COMICS Observations

HD165014 was observed with the COoled Mid-Infrared Camera and Spectrometer (COMICS; Kataza et al. 2000) mounted on the 8 m Subaru Telescope on 2008 July 16 and 17. Imaging observations in the $8.8\ \mu\text{m}$, $11.7\ \mu\text{m}$, and $18.8\ \mu\text{m}$ bands were carried out. The secondary mirror chopping method was used for the background cancellation. We used standard stars ($\gamma\ \text{Aql}$ and $\epsilon\ \text{Sco}$) from Cohen et al. (1999) as a flux calibrator and the reference point-spread functions were derived from the observations. We observed the standard stars before or after the observations of HD165014 in the same manner as HD165014. For the data reduction, we used our own reduction tools and IRAF (Tody 1993). The standard chop pair subtraction and the shift-and-add method in units of 0.1 pixel were employed. We applied airmass correction using ATRAN (Lord 1992). The derived flux densities are summarized in Table 1.

2.4. Photospheric Fitting

The photospheric flux density of HD165014 is estimated from the Kurucz model (Kurucz 1992) fitted to the *BVI*- and Two Micron All Sky Survey (Skrutskie et al. 2006) *JHK_s*-band photometry of the star taking account of the extinction. The only available spectral classification of HD165014 (F2V) is provided by the Michigan Catalog (Houk & Cowley 1975). We reexamine the spectral type of the star by the photospheric fitting. We use the Kurucz models of various spectral-type dwarfs for the stellar photospheric template of HD165014 and the distance d and the extinction A_V are set free. We adopt an extinction curve A_λ/A_V given by Fitzpatrick & Massa (2009),

$$\frac{A_\lambda}{A_V} = \left(\frac{0.349 + 2.087R_V}{1 + (\lambda/0.507)^{2.05}} - R_V \right) \frac{1}{R_V}, \quad (1)$$

where A_λ is the extinction toward the star at a wavelength λ (in μm) and the ratio of the total to the selective extinction R_V is assumed as 3.11.

The photospheric fitting shows that the *BVIJHK_s*-band photometry of HD165014 is well accounted for with almost the same significance by spectral types between B8V ($T_{\text{eff}} = 12000$ K) with $A_V = 3.0$ at $d = 190$ pc and F2V ($T_{\text{eff}} = 7000$ K) with $A_V = 1.9$ at $d = 70$ pc. It is difficult to determine the spectral type of the star more accurately only from photometric data due to its large extinction and optical high-resolution spectroscopy is required for further examination. An earlier spectral type at a larger distance seems more reasonable for HD165014, taking account of the large amount of extinction. In the following we assume A0V (with $A_V = 2.7$ and $d = 140$ pc) as the spectral type of HD165014 rather than F2V given by the Michigan Catalog. The estimated extinction $A_V = 2.7$ is still large for a star at 140 pc, suggesting that part of extinction may be of circumstellar origin. The derived photospheric flux density from the fitting in each MIR band, which does not depend on the spectral type sensitively (only a few percent of variation from B8V to F2V), is listed in Table 1.

3. Results

3.1. Spectral Energy Distribution

The obtained *Spitzer*/IRS spectrum of the star is shown in Figure 1 together with the *AKARI* and Subaru/COMICS photometry. The measurements of the *MSX* counterpart (MSX6C G009.0807+00.3009) and the *Spitzer*/IRAC GLIMPSE II counterpart (SSTGLMC G009.0801+00.3011) are also shown in Figure 1. Most of the MIR flux densities are in good

agreement with each other, while those of *AKARI* 18 μm band and *Spitzer*/IRAC 8 μm -band are slightly higher than the others. The expected photospheric emission is also plotted in Figure 1. Significant excess emission at wavelengths longer than 5 μm is clearly seen. The detected flux densities at 9 and 18 μm are 10 and 30 times larger than the photosphere, respectively, unambiguously indicating the presence of a warm and bright debris disk. The slope of the observed spectrum at $\lambda \gtrsim 20 \mu\text{m}$ is consistent with that of the Rayleigh-Jeans side of a blackbody, suggesting the dust temperature of $\gtrsim 300 \text{ K}$ and the truncation of the disk at the radius where the dust temperature is $\sim 300 \text{ K}$.

One of the observable indicators of dust abundance is its fractional luminosity, a ratio of the infrared luminosity from the disk to the stellar luminosity. The fractional luminosity of HD165014 is estimated as $\sim 5 \times 10^{-3}$. It is comparable to $\beta \text{ Pic}$ (Barrado y Navascués et al. 1999), suggesting that HD165014 is one of the brightest debris disks discovered so far. The location of the star, deep in the galactic plane, makes it difficult to find until the *AKARI* survey.

3.2. Features in the Spectrum of the Excess

To examine the excess emission, we subtract the expected photospheric emission from the observed IRS spectrum. The photosphere-subtracted spectrum shows significant emission features centered at around 10 and 20 μm . A ubiquitous dust species family, silicate, which has features around $\sim 10 \mu\text{m}$ (due to Si-O stretching modes) and $\sim 20 \mu\text{m}$ (due to O-Si-O bending modes), seems to be a main carrier of the observed features. Particularly, the spectrum shows several fine-structured features attributable to crystalline silicates.

To investigate the details of the features, Figure 2 plots the normalized emissivity of the excess emission of HD165014 by dividing the photosphere-subtracted spectrum by a blackbody ($B_\nu(T)$) of a temperature T , where T is chosen so that the spectrum level of the feature-free region (8.0 and 13.2 μm for the top panel, and 13.5 and 33 μm for the bottom panel of Figure 2) becomes almost flat. The chosen T is 560 and 330 K for the top and bottom panels of Figure 2, respectively. For comparison, spectra of crystalline enstatite, forsterite (Tamanai et al. 2006), and fused silica (Koike et al. 1989) are also plotted in Figure 2.

A significant broad feature is seen at 9–12 μm in the spectrum. Since the width of this feature is large (FWHM $\sim 2.8 \mu\text{m}$), it seems to originate from μm -sized amorphous silicate rather than sub- μm -sized silicate (van Boekel et al. 2003). In addition, some peaks are also seen on the broad feature. The most significant peak is located at 9.3 μm , and the second at 10.5 μm . Weaker narrow features are also seen around 11.1–11.5 μm . The positions of all the

narrow features are consistent with the spectrum of crystalline enstatite. The $9.8 \mu\text{m}$ feature of crystalline forsterite, which is the most common form of crystalline silicate, is not seen in the excess emission of HD165014. Only weak narrow features are seen around $11.1\text{--}11.5 \mu\text{m}$, where a strong crystalline forsterite feature is expected, in the spectrum of HD165014.

To analyze the N -band spectrum quantitatively and confirm the identification of the features described above, we make a simple spectral model fitting of the derived emissivity at $8\text{--}13 \mu\text{m}$. We consider four dust species, crystalline forsterite and enstatite (Tamanai et al. 2006) and amorphous olivine and pyroxene (Dorschner et al. 1995), in our model fit. The model spectrum is given by

$$\text{Emissivity} = a_{\text{cont}} + a_{\text{ol}}Q_{\text{ol}} + a_{\text{px}}Q_{\text{px}} + a_{\text{fo}}Q_{\text{fo}} + a_{\text{en}}Q_{\text{en}}, \quad (2)$$

where Q_{ol} , Q_{px} , Q_{fo} , and Q_{en} are the absorption efficiencies of amorphous olivine, amorphous pyroxene, crystalline forsterite, and crystalline enstatite, respectively. The scaling factors, a s, are free parameters (a_{cont} is the contribution of continuum). For amorphous olivine and pyroxene, we choose one dust size from 0.1 , 1.0 , 1.5 , or $2.0 \mu\text{m}$, whose absorption coefficients are computed from the optical constants of Dorschner et al. (1995) based the Mie theory (Bohren & Huffman 1983). We employ a least-squares minimization method to determine the most likely parameters. A model with $2.0 \mu\text{m}$ sized amorphous silicates is found to provide the best fit among all the considered dust sizes of amorphous silicates. The derived best-fit parameters are $a_{\text{cont}} = 0.44$, $a_{\text{ol}} = 0.00$, $a_{\text{px}} = 0.24$, $a_{\text{fo}} = 0.03$, and $a_{\text{en}} = 0.32$. The best-fit model spectrum is shown in the top panel of Figure 3, indicating that the N -band spectrum of HD165014 is well reproduced by the model spectrum. The broad and narrow features seen in the observed spectrum are indeed attributed to $2 \mu\text{m}$ sized amorphous pyroxene and crystalline enstatite, respectively. The contribution of forsterite dust is small and the mass ratio of forsterite to enstatite is estimated as $\sim 1/20$.

In the longer wavelength region of the spectrum, a significant trapezoidal feature is seen at $17\text{--}20 \mu\text{m}$, which is very similar to the enstatite spectrum. A broad feature seen around $28 \mu\text{m}$ also seems to originate from enstatite. A weak feature is seen around $23 \mu\text{m}$, which may be accounted for by both forsterite and enstatite. The feature around $23 \mu\text{m}$ might be attributable to forsterite; forsterite, if any, is less abundant than enstatite since the feature is very weak. Silica features at 9.0 and $20\text{--}21 \mu\text{m}$ are not seen in the excess emission of HD165014.

The observed features and their identifications are summarized in Table 2. From the overall shape of the MIR excess spectrum of HD165014, we conclude that most of the fine features are attributable to crystalline enstatite and that forsterite is much less abundant than enstatite around the star. The feature-to-continuum ratios in the 10 and $20 \mu\text{m}$ regions are ~ 1 and ~ 0.25 , respectively. The contribution from the continuum component is large

in the excess emission of HD165014, suggesting the presence of abundant featureless large dust grains ($> 10 \mu\text{m}$ in size) around the star.

3.3. Radial Distribution of Dust

In the top panel of Figure 2, a rising continuum toward shorter wavelengths $\lambda \lesssim 7 \mu\text{m}$ is seen, suggesting the presence of hotter ($T > 560 \text{ K}$) materials around the star. Although the rising continuum might also be attributable to amorphous carbon, whose emissivity rises toward shorter wavelengths in the NIR and MIR (Jager et al. 1998), no more discussion can be given with the present data. The temperature of the hottest component is estimated as $T = 750 \text{ K}$ from a fitting of the $5 - 7 \mu\text{m}$ excess spectrum with a single-temperature blackbody assuming that the $5 - 7 \mu\text{m}$ excess is coming from the innermost hottest region. Therefore dust grains are distributed in the region with temperatures of $T = 750 - 300 \text{ K}$ around HD165014. The inner and outer radii of the debris disk are estimated as 0.70 AU and 4.4 AU , respectively, by assuming that the debris dust is a blackbody particle. Possible large circumstellar extinction suggests that the disk is seen nearly edge-on.

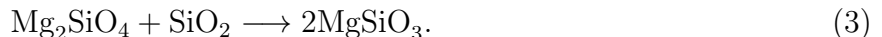
4. Discussion

As mentioned above, it is evident that crystalline enstatite is abundant in the debris disk around HD165014 and forsterite features are not clearly seen. Chen et al. (2006) conduct a comprehensive MIR spectroscopic survey of debris disks. Among their 59 debris disk samples, five objects (HR3927, $\eta \text{ Crv}$, HD113766, HR7012, and $\eta \text{ Tel}$) are found to possess spectral features that are well-modeled by μm -sized amorphous and crystalline silicates. Forsterite features are dominant compared to enstatite toward four samples (HR3927, $\eta \text{ Crv}$, HD113766, and $\eta \text{ Tel}$). HR7012, which shows a very strong peak at $9.1-9.2 \mu\text{m}$ in its spectrum, was initially modeled by enstatite-rich silicate by Chen et al. (2006). However, Lisse et al. (2009) conclude that the observed $9.1-9.2 \mu\text{m}$ feature originates from abundant silica grains and that the feature strengths of enstatite and forsterite are almost comparable. Although there are a few additional debris disk stars with significant dust features in the N -band ($\beta \text{ Pic}$, HIP8920, HD145263; Knacke et al. 1993; Song et al. 2005; Honda et al. 2004), no sample with high abundance of enstatite is reported to date. HD165014 is the only known debris disk that shows strong enstatite features compared to forsterite.

In the solar system, a number of achondrite meteorites, which are primarily composed of enstatite, named Aubrites, have been discovered. E-type asteroids are thought to have en-

statite achondrite surfaces and to be parent bodies of aubrites (e.g. Zellner et al. 1977) based on their reflection spectra. E-type asteroids form a large proportion of asteroids inward of the main belt known as Hungaria asteroids and are believed to be fragments of differentiated larger bodies that were heated at least to 1700 K (Keil et al. 1989). Considering that enstatite is dominant around HD165014 rather than forsterite, the observed debris dust may originate from an analog of E-type asteroids in the solar system, being harmonic with the idea that the debris disk is formed by means of collisions between asteroids (Backman & Paresce 1993). It is also known that Mercury’s surface is rich in enstatite (Sprague & Roush 1998). If a Mercury-like planet exists around HD165014 and a mechanism to scatter the surface material of the planet, for example infall of small bodies, occurs, an enstatite-rich debris disk might be formed. It should also be noted that Mercury’s high density is interpreted as a result of stripping of the surface crustal material (Benz et al. 1988). The possible link between the debris material around HD165014 and Mercury needs to be further explored.

Although a number of MIR spectra of protoplanetary disks associated with younger stars, Herbig Ae/Be and T Tau stars, have been collected so far, objects that show enstatite features are rare. HD179218 is a Herbig Ae/Be star, which has the most enstatite-rich spectrum known to date (Bouwman et al. 2001; Schütz et al. 2005). We show the *N*-band spectrum of HD179218 obtained with TIMMI2 (van Boekel et al. 2005) in the bottom panel of Figure 3. While crystalline enstatite features are clearly seen in the spectrum, features at 9.85 and 11.20 μm attributable to forsterite are also seen with comparable strengths as enstatite, suggesting the presence of abundant crystalline forsterite as well as enstatite. Annealing experiments of a magnesium silicate smoke made by Rietmeijer et al. (1986) show that the initially formed forsterite and silica react with each other and form enstatite by the following reaction



Bouwman et al. (2001) suggest that the presence of enstatite around HD179218 might be due to the high luminosity ($300L_\odot$), which gives rise to rapid dispersal of the gas, resulting in a high efficiency of the reaction. van Boekel et al. (2005) suggest that enstatite might be produced by means of chemical equilibrium processes in high temperature environments, i.e., inner regions of the protoplanetary disk. Sato et al. (2006) show that crystalline enstatite can be produced by simultaneous evaporation of SiO grains and Mg vapor in a plasma in laboratory experiments. It is now widely accepted that the turbulence in disks is attributed to the magnetorotational instability (MRI; Balbus & Hawley 1991), suggesting that at least part of the disk is sufficiently ionized (e.g. Inutsuka & Sano 2005). Therefore the formation process of crystalline enstatite suggested by Sato et al. (2006) may work efficiently in protoplanetary disks. It is possible that crystalline enstatite grains produced in the protoplanetary disk were once stored in small bodies such as comets and have been released recently in the HD165014

system. Indeed crystalline enstatite is detected toward some comets in the solar system by astronomical MIR observations (e.g. Lisse et al. 2006) as well as by the STARDUST sample return mission (e.g. Zolensky et al. 2006). However, it remains an open question why crystalline forsterite is depleted around HD165014. Further experimental and theoretical studies are required to discuss the origin of abundant crystalline enstatite in the debris disk around HD165014 in detail.

This research is in part based on observations with *AKARI*, a JAXA project with the participation of ESA. It is also based on observations with *Spitzer*, which is operated by the Jet Propulsion Laboratory, California Institute of Technology, under a contract with NASA, and with Subaru Telescope, which is operated by the National Astronomical Observatory of Japan. We thank A. Tamanai for providing us with silicate spectra, R. van Boekel for providing us with Herbig Ae/Be spectra, and the anonymous referees, M. Honda, Y. K. Okamoto, C. M. Lisse, H. Chihara, Y. Imai, A. Takigawa, D. Kato, and H. Kimura for their useful comments and suggestions. This research was supported by the MEXT, “Development of Extrasolar Planetary Science.” H. F. is supported by the JSPS.

Facilities: *AKARI* (ISAS/JAXA), *Spitzer* (NASA), Subaru (NAOJ).

REFERENCES

- Backman, D. E., & Paresce, F. 1993, *Protostars and Planets III*, ed. E. H. Levy & J. I. Lunine (Tucson, AZ: Univ. Arizona Press), 1253
- Balbus, S. A., & Hawley, J. F. 1991, *ApJ*, 376, 214
- Benz, W., Slattery, W. L., & Cameron, A. G. W. 1988, *Icarus*, 74, 516
- Barrado y Navascués, D., Stauffer, J. R., Song, I., & Caillault, J.-P. 1999, *ApJ*, 520, L123
- Bohren, C. F., & Huffman, D. R. 1983, *Absorption and Scattering of Light by Small Particles* (New York: Wiley)
- Bouwman, J., Meeus, G., de Koter, A., Hony, S., Dominik, C., & Waters, L. B. F. M. 2001, *A&A*, 375, 950
- Chen, C. H., et al. 2006, *ApJS*, 166, 351
- Cohen, M., Walker, R. G., Carter, B., Hammersley, P., Kidger, M., & Noguchi, K. 1999, *AJ*, 117, 1864

- Dorschner, J., Begemann, B., Henning, T., Jaeger, C., & Mutschke, H. 1995, *A&A*, 300, 503
- Fitzpatrick, E. L., & Massa, D. 2009, *ApJ*, 699, 1209
- Fujiwara, H., et al. 2010, *A&A*, submitted
- Honda, M., et al. 2004, *ApJ*, 610, L49
- Houk, N., & Cowley, A. P. 1975, *Michigan Catalog of Two-dimensional Spectral Types for HD Stars, Vol. 1* (Ann Arbor, MI: Univ. Michigan Dept. Astron.)
- Houck, J. R., et al. 2004, *ApJS*, 154, 18
- Inutsuka, S., & Sano, T. 2005, *ApJ*, 628, L155
- Ishihara, D., et al. 2010, *A&A*, in press (arXiv:1003.0270)
- Jager, C., Mutschke, H., & Henning, T. 1998, *A&A*, 332, 291
- Kataza, H., Okamoto, Y., Takubo, S., Onaka, T., Sako, S., Nakamura, K., Miyata, T., & Yamashita, T. 2000, *Proc. SPIE*, 4008, 1144
- Keil, K., Ntaflou, T., Taylor, G. J., Brearley, A. J., & Newsom, H. E. 1989, *Geochim. Cosmochim. Acta*, 53, 3291
- Knacke, R. F., Fajardo-Acosta, S. B., Telesco, C. M., Hackwell, J. A., Lynch, D. K., & Russell, R. W. 1993, *ApJ*, 418, 440
- Koike, C., Komatuzaki, T., Hasegawa, H., & Asada, N. 1989, *MNRAS*, 239, 127
- Kurucz, R. L. 1992, in *IAU Symp. 149, The Stellar Populations of Galaxies*, ed. B. Barbuy & A. Renzini (Dordrecht: Kluwer), 225
- Lecavelier Des Etangs, A., Vidal-Madjar, A., & Ferlet, R. 1996, *A&A*, 307, 542
- Lisse, C. M., Chen, C. H., Wyatt, M. C., Morlok, A., Song, I., Bryden, G., & Sheehan, P. 2009, *ApJ*, 701, 2019
- Lisse, C. M., et al. 2006, *Science*, 313, 635
- Lord, S. D. 1992, *A New Software Tool for Computing Earth's Atmospheric Transmission of Near- and Far-Infrared Radiation* (NASA Tech. Memo 103957; Washington, DC: NASA)
- Murakami, H., et al. 2007, *PASJ*, 59, 369

- Onaka, T., et al. 2007, PASJ, 59, 401
- Rietmeijer, F. J. M., Nuth, J. A., & MacKinnon, I. D. R. 1986, Icarus, 66, 211
- Sato, T., et al. 2006, Planet. Space Sci., 54, 617
- Schütz, O., Meeus, G., & Sterzik, M. F. 2005, A&A, 431, 165
- Song, I., Zuckerman, B., Weinberger, A. J., & Becklin, E. E. 2005, Nature, 436, 363
- Skrutskie, M. F., et al. 2006, AJ, 131, 1163
- Sprague, A. L., & Roush, T. L. 1998, Icarus, 133, 174
- Tamanai, A., Mutschke, H., Blum, J., & Meeus, G. 2006, ApJ, 648, L147
- Tody, D. 1993, in ASP Conf. Ser. 52, Astronomical Data Analysis Software and Systems II, ed. R. J. Hanisch, R. J. V. Brissenden, & J. Barnes (San Francisco, CA: ASP), 173
- van Boekel, R., Min, M., Waters, L. B. F. M., de Koter, A., Dominik, C., van den Ancker, M. E., & Bouwman, J. 2005, A&A, 437, 189
- van Boekel, R., Waters, L. B. F. M., Dominik, C., Bouwman, J., de Koter, A., Dullemond, C. P., & Paresce, F. 2003, A&A, 400, L21
- Werner, M. W., et al. 2004, ApJS, 154, 1
- Zellner, B., Leake, M., Williams, J. G., & Morrison, D. 1977, Geochim. Cosmochim. Acta, 41, 1759
- Zolensky, M. E., et al. 2006, Science, 314, 1735

Table 1: Infrared Photometry of HD165014.

λ (μm)	F_ν (Jy)	Instrument	Photosphere ^a (Jy)	Significance, χ ^b
5.8	0.90 ± 0.02	<i>Spitzer</i> /IRAC ^c	0.26	27
8.0	1.06 ± 0.02	<i>Spitzer</i> /IRAC ^c	0.14	43
8.28	1.08 ± 0.05	<i>MSX</i> ^d	0.14	22
8.8	0.93 ± 0.09	COMICS	0.12	10
9	1.36 ± 0.10	<i>AKARI</i> /IRC	0.14	13
11.7	0.89 ± 0.09	COMICS	0.069	10
12.13	0.78 ± 0.07	<i>MSX</i> ^d	0.064	11
14.65	0.76 ± 0.06	<i>MSX</i> ^d	0.044	13
18	0.96 ± 0.14	<i>AKARI</i> /IRC	0.030	7
18.8	0.84 ± 0.01	COMICS	0.027	220

^aFrom the Kurucz model to fitted to *BVIJHK_s*-bands data.

^b $\chi = (\text{Observed} - \text{Kurucz})/\text{noise}$.

^cThe *Spitzer* GLIMPSE II counterpart (SSTGLMC G009.0801+00.3011), whose positional offset from HD165014 is $0''.10$. See <http://www.astro.wisc.edu/glimpse/glimpsedata.html>.

^dThe *MSX* counterpart (*MSX6C* G009.0807+00.3009), whose positional offset from HD165014 is $2''.58$.

Table 2: Features in Excess Emission of HD165014.

λ (μm)	Comment	Identification
10 (7.3–12.4)	Very strong broad feature	Silicate
9.3	Strong peak within 10 μm feature	Crystalline En
10.5	Strong peak within 10 μm feature	Crystalline En
11.1	Peak within 10 μm feature	Crystalline En/Fo
11.5	Shoulder within 10 μm feature	Crystalline En
14.0–15.0	Weak feature	Unidentified
18 (17.8–19.7)	Strong trapezoidal emission	Crystalline En
22.8–24.3	Weak feature	Crystalline En/Fo
27.3–30.3	Weak feature	Crystalline En
33.8–34.5	Possible weak feature, low signal-to-noise ratio	Unidentified

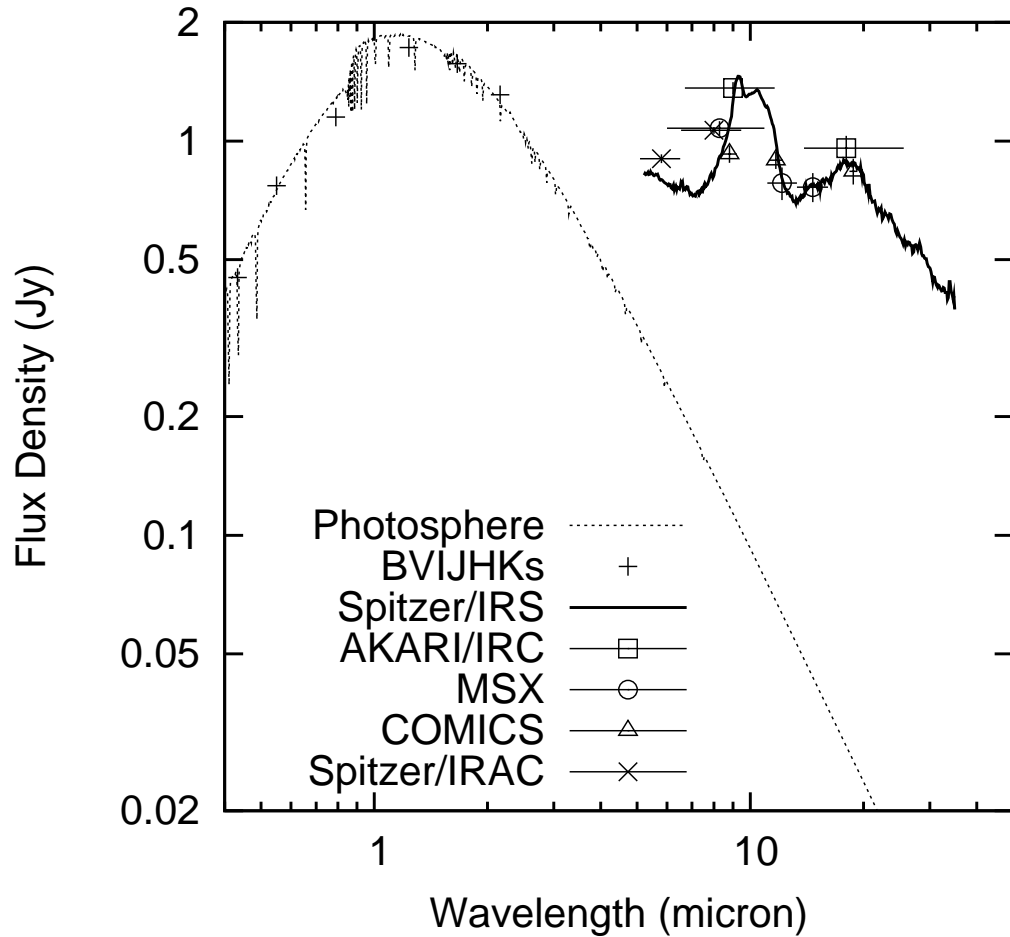


Fig. 1.— Spectral energy distribution of HD165014. The open squares, triangles, circles, crosses, and pluses indicate the photometric data obtained with *AKARI/IRC*, *Subaru/COMICS*, *MSX*, *Spitzer/IRAC*, and *BVIJHK_S*-band photometry taken from Vizier database, respectively. The solid and dotted lines indicate the *Spitzer/IRS* spectrum and the photospheric contribution of an A0V star (Kurucz 1992), respectively.

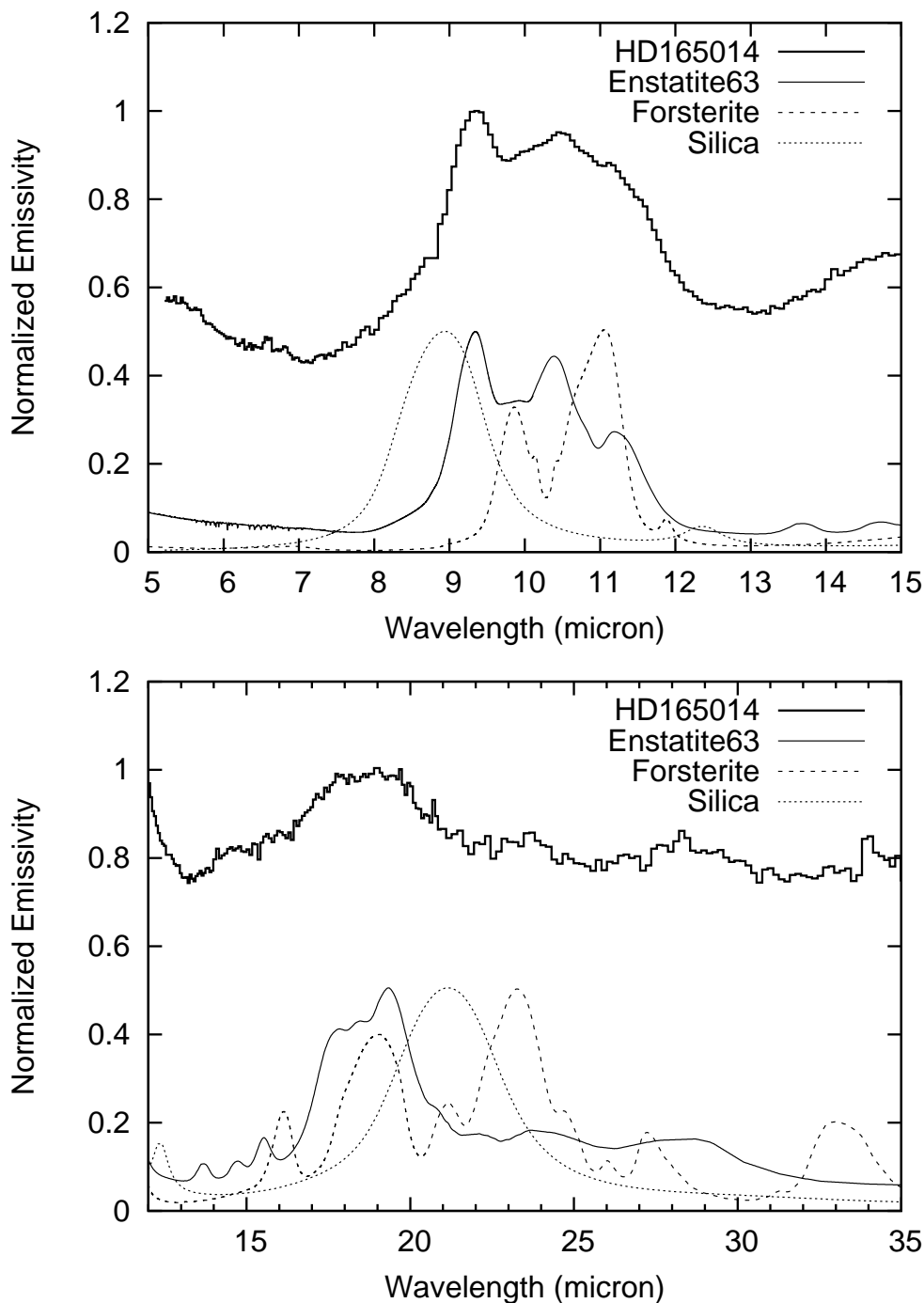


Fig. 2.— Top: emissivity of the excess emission of HD165014 at 5–15 μm derived by division of the observed spectrum by a blackbody of $T = 560$ K (thick solid line). For comparison, spectra of crystalline enstatite, forsterite, and fused silica from laboratory measurements are also plotted as thin solid, dashed, and dotted lines, respectively. Bottom: emissivity of the excess emission of HD165014 at 12–35 μm derived by division of the observed spectrum by a blackbody of $T = 330$ K. The line styles are the same as the top panel.

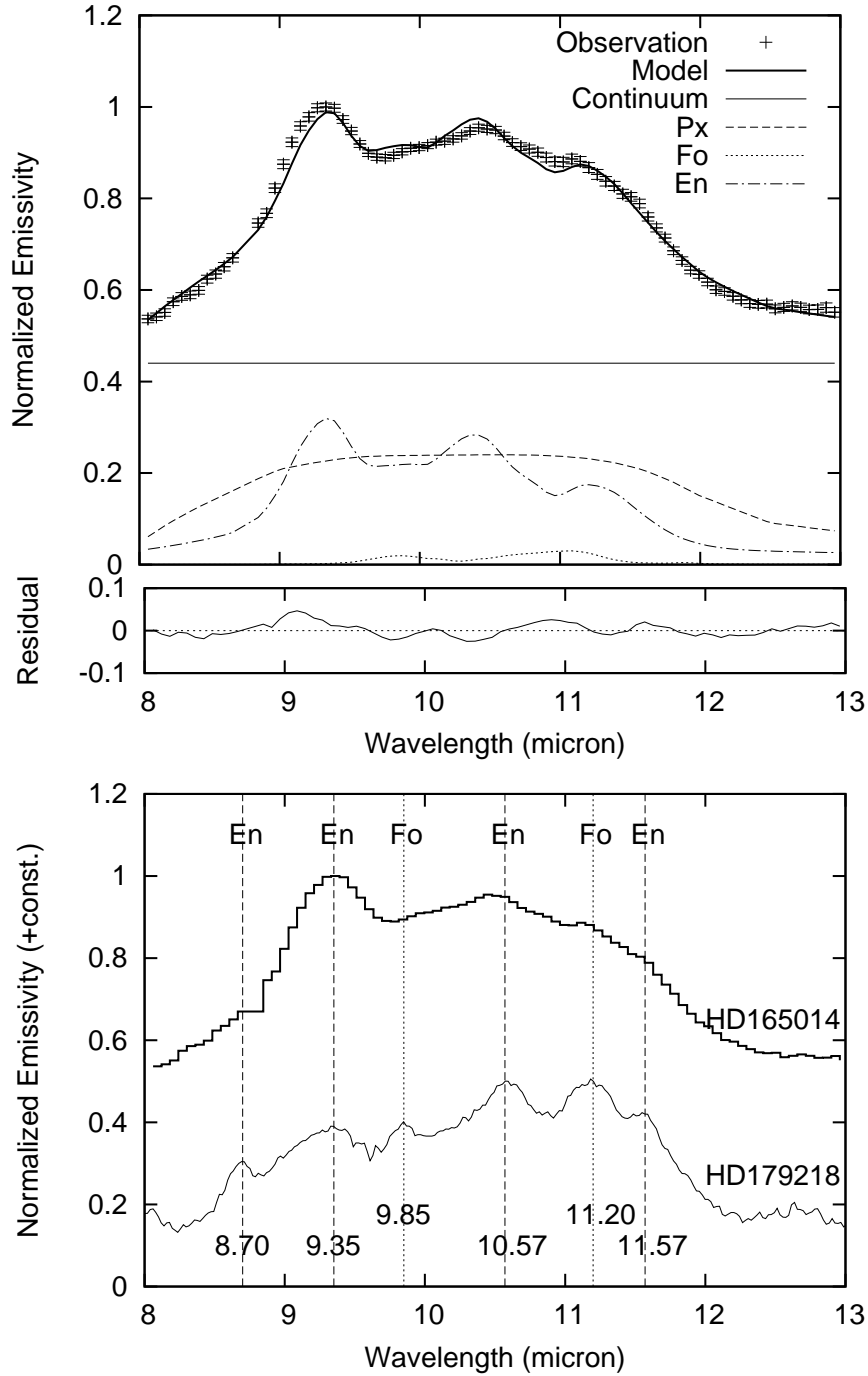


Fig. 3.— Top: fit result of the N -band emissivity of HD165014. The thick solid line is the best-fit model spectrum, which is the sum of constant continuum (thin solid line), 2.0 μm -sized amorphous pyroxene (dashed line), crystalline forsterite (dotted line), and enstatite (dot-dashed line). Amorphous olivine component is not shown since no contribution of it is required in the best-fit model. The residual spectrum subtracted by the best-fit model is shown below the fit result. Bottom: comparison of the N -band spectra of HD165014 (thick solid line) and enstatite-rich Herbig Ae/Be star HD179218 (thin solid line; van Boekel et al. 2005). The vertical dashed and dotted lines indicate peak positions of crystalline enstatite (En) and forsterite (Fo) detected toward HD179218, respectively.